Appl Phys A (2008) 92: 531–539
DOI 10.1007/s00339-008-4606-z

Applied Physics A
Materials Science & Processing

RAPID COMMUNICATION

The feasibility of producing MWCNT paper and strong MWCNT film from VACNT array

Guanghui Xu · Qiang Zhang · Weiping Zhou · Jiaqi Huang · Fei Wei

Received: 22 April 2008 / Accepted: 25 April 2008 / Published online: 14 May 2008

Abstract This study sought to produce carbon nanotube (CNT) pulp out of extremely long, vertically aligned CNT arrays as raw materials. After high-speed shearing and mixing nitric acid and sulfuric acid, which served as the treatment, the researchers produced the desired pulp, which was further transformed into CNT paper by a common filtration process. The paper's tensile strength, Young's modulus and electrical conductivity were 7.5 MPa, 785 MPa and 1.0×10^4 S/m, respectively, when the temperature of the acid treatment was at 110°C. Apart from this, the researchers also improved the mechanical property of CNT paper by polymers. The CNT paper was soaked in polyethylene oxide, polyvinyl pyrrolidone, and polyvinyl alcohol (PVA) solution, eventually making the CNT/PVA film show its mechanical properties, which increased, while its electrical conductivity decreased. To diffuse the polymer into the CNT paper thoroughly, the researchers used vacuum filtration to fabricate a CNT/PVA film by penetrating PVA into the CNT paper. After a ten-hour filtration, the tensile strength and Young's modulus of CNT/PVA film were 96.1 MPa and 6.23 GPa, respectively, which show an increase by factors of 12 and 7, respectively, although the material's electrical conductivity was lowered to 0.16×10^4 S/m.

PACS 81.40.Rs · 81.05.Uw · 81.05.Qk · 81.07.De · 82.35.Np

G. Xu · Q. Zhang (✉) · W. Zhou · J. Huang · F. Wei
Beijing Key Laboratory of Green Chemical Reaction Engineering and Technology, Department of Chemical Engineering, Tsinghua University, Beijing 100084, China
e-mail: zhang-qiang@mails.tsinghua.edu.cn

F. Wei
e-mail: weifei@flotu.org

1 Introduction

Carbon nanotubes (CNTs) have become the focus of nanoscience and nanotechnology for many years due to their special structures and exceptional properties [1–4]. Until now, various CNT macroscopic structures, including CNT array [1, 2], CNT yarn [4], CNT paper [5–15], CNT films [16–20], CNT sheet [21], CNT membrane [22] and CNT fibres [23], have been reported. The CNT paper or buckypaper has excellent electrical and mechanical properties [5–22], thus attracting wide use in many applications, including actuators, sensors, capacitors, electrodes, fuel cell, and field emission devices. Recently, Pushparaj et al. [24] reported on CNT-based composite papers, which were ultrathin, flexible, safe energy storage devices to meet various design and power needs of modern gadgets. CNT papers usually have an electrical conductivity of 10^4–10^5 S/m and tensile strength of 10–80 MPa [5–22].

Meanwhile, most CNT papers are made of single-walled CNTs (SWCNTs). However, compared with multiwalled CNTs (MWCNTs), SWCNTs are expensive; moreover, the purification and dispersion of SWCNTs in gas or liquid are still difficult. MWCNTs are always in an agglomerated form [25]. After being dispersed further by ball milling and acid treatment, MWCNTs obtained an aspect ratio of less than 1,000 [26], which cannot be easily transformed into CNT paper. Recently, it was shown that vertically aligned MWCNT (VACNT) arrays consisting mainly of CNTs with good alignment and large aspect ratio can be obtained in a large amount [27–29]. The length of CNT in array form can reach 6.0 mm, and the aspect ratio is above 10^5. Moreover, the entanglements of CNTs in array form are much less than those in agglomerated CNTs. Recently, Wang et al. [30] directly used VACNT arrays to fabricate oriented CNT papers. However, the size of CNT paper was limited.

In this study, VACNT arrays were dispersed by high-speed shearing, acid treatment, and pulping. After filtering the CNT pulp, the researchers produced CNT paper, whose mechanical and electrical properties were then tested. The paper was strengthened further with various polymers by soaking or vacuum filtration. The properties of the composite film were also identified and reported.

2 Experimental

2.1 Synthesis, dispersion, and functionalization of VACNT arrays

In this study, VACNT arrays, which were about 5.0 mm long after 150-minute growth (see Fig. 1a), were synthesized by floating catalysis process [27–29]. The VACNT arrays were not easy to hold together as a large-area film; apart from this, strong anisotropies also appeared. Along the axis direction, VACNT arrays were easily torn into small bundles. Then the VACNT arrays were sheared into CNT cotton by high-speed shearing. CNT cotton was further functionalized by mixed-acid treatment. The process was done by adding 0.3 g CNT cotton, 15 ml nitric acid, and 45 ml sulfuric acid in a 100 ml Teflon reactor. The temperature of the reactor was controlled by temperature programming equipment. The temperature was raised from room temperature to 90°C in 30 minutes, kept constant at 90°C for 30 minutes, then naturally cooled down to room temperature. Various CNT samples were obtained by altering the constant temperature to 100, 110, 120, and 130°C. Then five VACNT array samples were obtained; they were named CNTs-90, CNTs-100, CNTs-110, CNTs-120, and CNTs-130 according to the temperature of the acid treatment.

2.2 CNT paper by filtration

Each sample was diluted to 300 ml using deionized water. The CNT solution was then stirred in an A-88 tissue triturator for two minutes, thus producing CNT pulp. This CNT pulp was a solution of long and well-dispersed CNTs. Furthermore, the CNT pulp was filtered through a microporous filter membrane (with a diameter of 6.5 cm and a pore diameter of 0.22 μm). When the pH value of the filtrate reached 7.0, the filtration stopped. After removing the acid, the researchers easily separated the CNT paper from the microporous filter membrane.

2.3 CNT/polymer composite film

To improve the property of the CNT paper further, the researchers used polymers to make a composite film by soaking or further filtration. Here, polyvinyl alcohol (PVA, purity ~97.0%, M_w of 75,000–79,000 g/mol), polyvinyl pyrrolidone (PVP, M_w of 90,000 g/mol), and polyethylene oxide (PEO, M_w of 58,000 g/mol), purchased from Beijing Yili Fine Chemicals Ltd., were used. The polymers were dissolved in deionized water to dissolve into a 1 wt% solution. The composite film was produced using the following procedure.

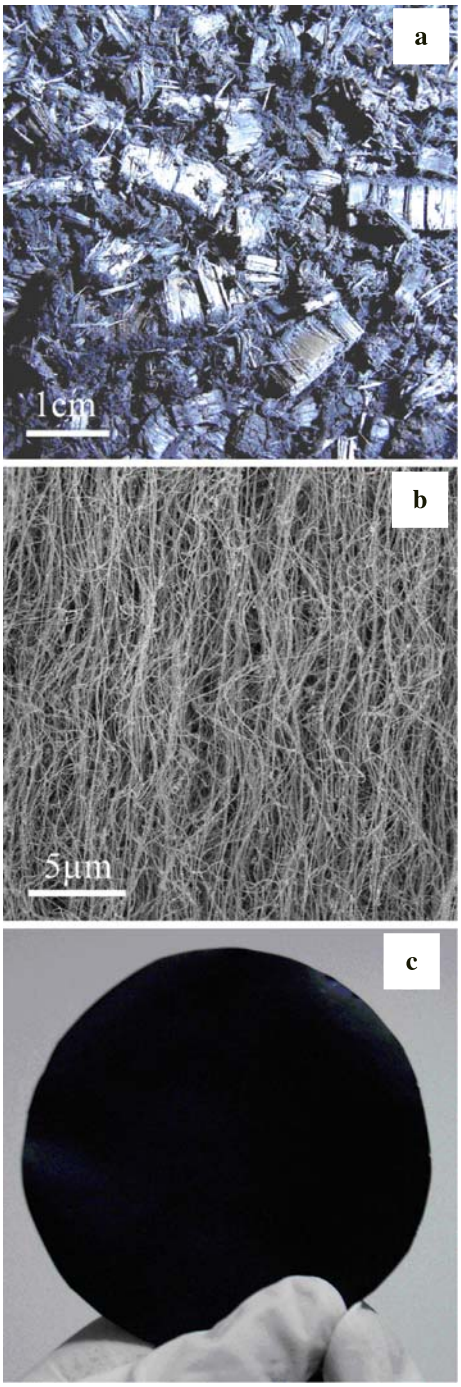

Fig. 1 The macroscopic (**a**) and SEM (**b**) images of as-grown VACNT arrays by the floating catalysis process. CNT paper was obtained as shown in (**c**)

2.3.1 *Soaking method*

The as-prepared CNT paper was simply soaked in 1 wt% polymer solution for three hours, 26 hours, and 72 hours. The film was then immersed in deionized water for one hour, compacted, and dried in an oven at 100°C for 30 minutes.

2.3.2 *Vacuum filtration method*

The CNT paper was kept on the filter. Then 1 wt% PVA solution was filtered through the paper. The filtration time was varied from 30 minutes, 10 hours, to 24 hours. Then the CNT films were separated from the microporous filter membrane, further compacted, and dried at 100°C for 30 minutes.

2.4 Characterization

The morphology of VACNT arrays was characterized by scanning electron microscopy (SEM, JSM 7401F at 3.0 kV). For transmission electron microscopy (TEM), about 5 mg of material was sonicated in ethanol, and several drops were put onto a TEM grid. The quality of the sample was characterized by high-resolution TEM (HRTEM, JEM 2010 at 120.0 kV). Raman experiments were performed with a Raman spectrophotometer Renishaw, RM2000 in ambient conditions. The spectra were recorded using a He-Ne laser excitation line of 633 nm. The infrared spectra of the mixed-acid treated VACNT arrays were measured by NEXUS FT-IR of Nicolet.

The mechanical properties of the films were tested using GT-TS-2000 Micro computational tensile testing machine (Taiwan Gaotie). The tested sample was 0.5 mm wide, 6.0 mm long, and approximately 0.1 mm thick. The stretching rate was 10.0 mm/min. At the least, five samples were tested, and the results were averaged. The volume resistivity was tested by four-probe dc measurement.

3 Results and discussion

3.1 CNT paper obtained by filtration

VACNT arrays were synchronously grown on the substrate by floating catalysis process [27–29]. When the growth time was 2.5 hours, the length of the VACNT arrays reached 5.0 mm (see Fig. 1a). The CNTs showed good alignment even when they were peeled from the substrate (see Fig. 1b). The density of VACNT array was about 20.0 g/L, which was further modulated by controlling the growth parameter. Then high-speed shearing was used to tear the VACNT arrays into small bundles. After a two-minute shearing, the VACNT arrays were dispersed into CNT cotton, which was CNT bundles with a diameter of ~1–10 μm and an apparent density of 2.0 g/L. Meanwhile, the length of CNT did not change much; the arrays were just torn into various bundles. The CNT cotton was then treated with nitric and sulfuric acids; this was done to remove catalysts, functionalize the surface of the CNTs, and obtain CNT pulp. At the same time, some CNTs were shortened. After dilution and washing, the CNT pulp was filtered. The solvent went through the filter membrane, and the CNTs were trapped. They stacked up together and entangled with each other; then CNT paper was produced (see Fig. 1c). As was apparent, the paper could be peeled down easily from the filter membrane. The size of the CNT paper depended upon the size of filter, and the thickness was determined by the amount of CNTs in the pulp. The surface of the CNT paper was smooth. The CNTs were mainly over several hundred micrometers to millimeters long, and thus the CNTs were with large aspect ratio and could be transformed into paper form easily.

The morphology of the CNT paper is shown in Fig. 2. A large amount of extra long CNTs randomly spread in the paper. Because the VACNT arrays were highly pure and because no surfactants were used during the dispersion, no other impurities, such as catalyst carriers and carbon spheres, were found in the CNT paper (see Fig. 2). As for the surface of the CNT paper, most of the CNTs were parallel in the surface and entangled with each other. Moreover, no obvious single CNT or CNT bundle was stretched out of the surface. Figure 2(b) shows that most of the CNTs were kept in a relative straight morphology, with a tortuosity factor of 1.14 ± 0.06 at a scale of 10 μm [31]. Unlike SWCNTs, the van der Waals force was not effective for MWCNT bundle formation. Thus, the MWCNTs were almost in individual state. The CNT paper was porous, showing the possibility for gas selective penetration. As shown in Fig. 2c, the CNT paper was a multilayered structure with each layer about 10 μm thick, while its total thickness was about 150 μm. The interface of each layer was not obvious. At the cross-section, the CNTs were stretched out into bundles during the stretch test. Some CNTs were obviously oriented after stretching, as shown in Fig. 2d.

Various applications have been proposed for buckypaper in the literature. However, most CNT papers were fabricated using SWCNTs as raw material. In this study, the MWCNTs in array form had an extremely large aspect ratio, from which MWCNT paper could be derived. However, the as-grown MWCNTs showed inert surface. Acid treatment was needed to enhance the interaction of CNTs. Because the temperature of the acid treatment affected the functionalization of MWCNTs obviously, the researchers varied it from 90 to 130°C. Some organic groups, including the carboxyl group, grafted at the surface and ends of CNTs. In the infrared spectra, as shown in Fig. 3, the peak at 1747.2 cm^{-1} increased obviously, indicating the graft of carboxyl groups.

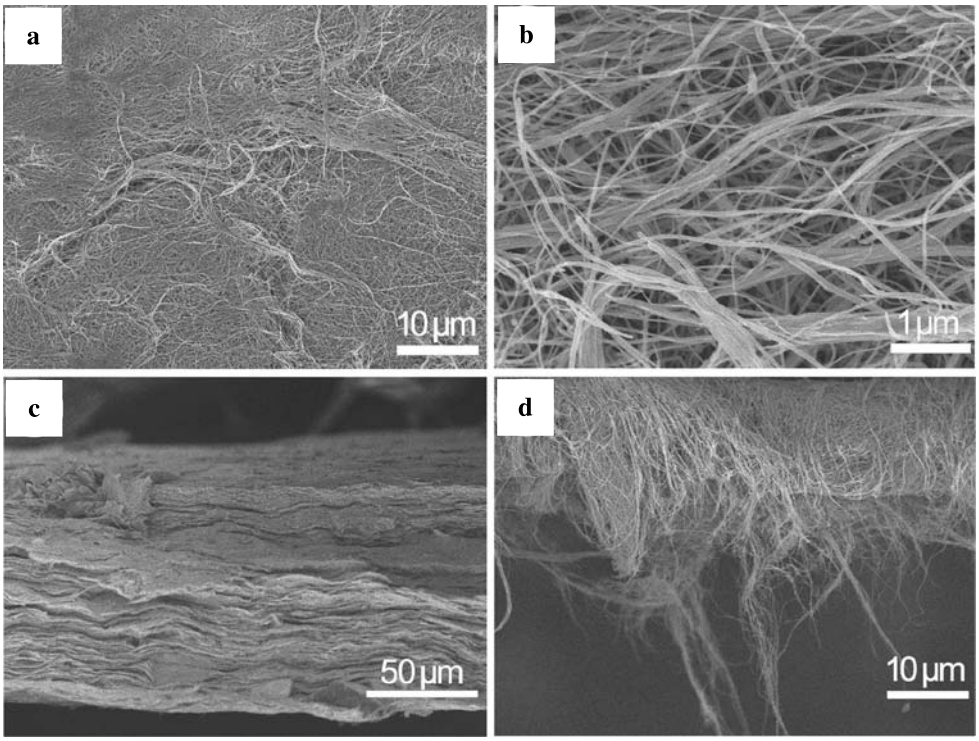

Fig. 2 SEM images of CNT paper obtained by filtration of CNT pulp. (**a**) and (**b**) show the surface of CNT paper; (**c**) and (**d**) show the cross-section of CNT paper

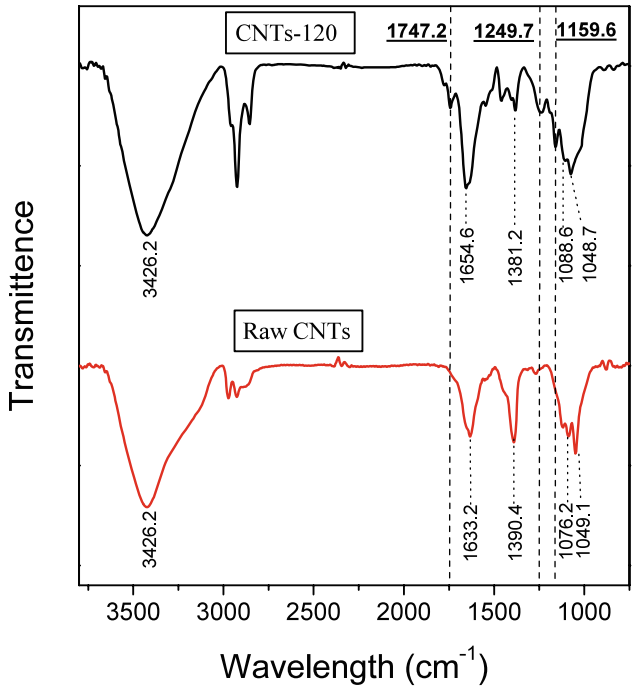

Fig. 3 The infrared spectra of CNTs before and after mixed acid treatment at 120°C for 0.5 hour

Meanwhile, the defect density of the paper increased, which can be confirmed by Raman spectra (Fig. 4) and HRTEM images (Fig. 5). The Raman spectrum is an important way to characterize the defect densities of carbon products macroscopically. Here, the ratio of intensity of D peak to G peak (I_D/I_G) can be used to characterize the degree of defect of MWCNTs [32]. The I_D/I_G ratio of raw MWCNTs was about 0.64, while the I_D/I_G ratio of acid-treated CNTs increased sharply as shown in Fig. 4a. When the acid treatment temperature was 90, 100, and 110°C, the I_D/I_G ratio was near 1.25. When the acid treatment temperature was increased further, the ratio increased to 1.40 (Fig. 4b). This shows that during the mixed-acid treatment, the carbon atoms at the surface were oxidized to carboxyl and hydroxyl groups, and the ordered graphite layers were destroyed [33, 34]. The etching effects were reinforced as the treatment temperature increased, thus increasing the I_D/I_G ratio. The HRTEM images shown in Fig. 5 also confirm that the graphite layers were significantly breached by the mixed acid. Both the end (Fig. 5a) and the side wall (Fig. 5b) of MWCNTs were etched. The ordered graphite layers were etched into discontinuous layers. Some carbon atoms were etched out by the attack of NO_2^+ in nitric acid and sulfuric acid, thus validating the results of prior studies [33, 34].

Various pieces of CNT paper were obtained from the CNT pulp by varying acid treatment temperature. The mechanical and electrical properties of CNT paper are listed in Table 1. The paper showed a tensile strength and Young's modulus over 4.3 and 426 MPa, respectively. When the acid treatment temperature increased, more carboxyl and hydroxyl groups were grafted, leading to strong interactions especially hydrogen-bond force among CNTs, thus increas-

ing tensile strength. As for the CNT paper obtained from CNTs-110, it had a tensile strength of 7.5 MPa and Young's modulus of 785 MPa. When the acid treatment temperature was higher, the defect density, which was indicated by the Raman spectra (Fig. 4) and HRTEM images (Fig. 5), considerably increased. Some CNTs were shortened, the aspect ratio of CNT decreased, and the mechanical properties were lowered. Compared with the data in Table 2, the results of electrical properties in this study were in the same order; furthermore, similar trends were shown as the mechanical properties. When the acid treatment temperature increased from 90 to 100°C, more functional groups will be grafted on the CNTs. Picozzi et al. reported that the new groups increased the number of bands near the Fermi level, promoting electron transfer between the carbon atoms [35]. Thus, the electrical conductivity was increased to 1.0×10^4 S/m since the CNT paper derived from CNTs-100 contained more functional groups than that derived from CNTs-90, which was similar to Lau's results [36]. However, when the acid treatment temperature increased further, the defect density revealed by the Raman spectra (Fig. 4) and TEM images (Fig. 5) considerably increased; meanwhile, some CNTs were shortened to be with a decreased aspect ratio, leading to gradual decrease of electrical conductivity. As a result of SWCNT functionalization leading to imper-

Table 1 The mechanical and electrical properties of CNT papers

Treatment temperature (°C)	Tensile strength (MPa)	Young's modulus (MPa)	Electrical conductivity (S/m)
90	4.3	426	0.83×10^4
100	4.6	439	1.0×10^4
110	7.5	785	1.0×10^4
120	6.0	557	0.91×10^4
130	4.5	455	0.91×10^4

Table 2 The mechanical and electrical properties of buckypapers in the literature

Type of CNTs	Process	Electrical conductivity (S/m)	Tensile strength (MPa)	Young's modulus (GPa)	Ref
SWCNT		5×10^4			[37]
SWCNT		4×10^4			[38]
SWCNT		6.67×10^3–2×10^4			[39]
SWCNT			10	1.2	[5]
SWCNT	oleum	1.30×10^5			[40]
	oleum, heat treated	9×10^4	30	8	
SWCNT	10M HNO_3	1.2×10^4	74	5	[17]
SWCNT			14–35	0.2–2	[41]
SWCNT	pristine	5.50×10^4			
	$SOCl_2$	3.00×10^5			
	H_2SO_3	1.46×10^5			[42]
	iodine	1.45×10^5			
	H_2SO_4	9.00×10^4			
	SO_2Cl_2	8.20×10^4			
SWCNT	pristine	7.00×10^4	11	0.66	[43]
	$SOCl_2$	3.50×10^5	37	0.95	
SWCNT	ionic liquid		16	2	[7]
SWCNT	Triton X-100	2.47×10^4	16	4	
	DNA	3.06×10^4	76	3.3	[44]
	chitosan	2.90×10^4	149	3.4	
SWCNT	pristine	3.03×10^3			
	ozonized	3.23×10^2			[45]
	CdTe decorated	7.14×10^2			
DWCNT			680–850	10.8–12.2	[18]
DWCNT		9.09×10^5–2×10^6			[19]
MWCNT		1.1×10^4–2.0×10^4			[30]

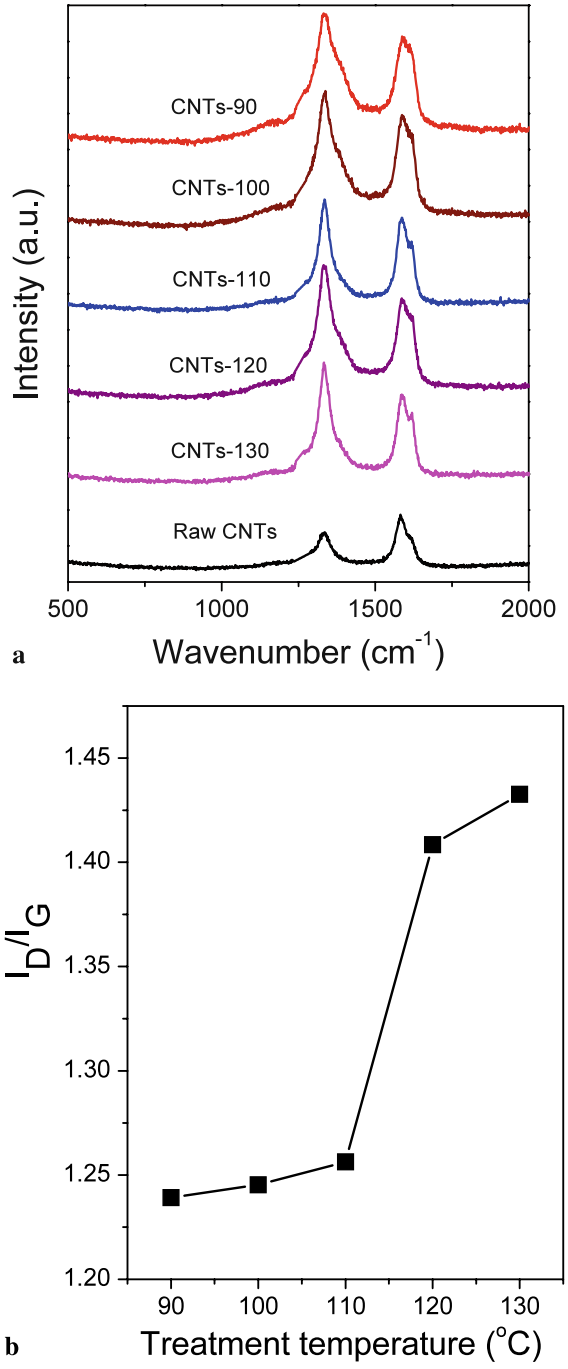

Fig. 4 (**a**) The Raman spectra of VACNT arrays before and after mixed-acid treatment. (**b**) The relationship between I_D/I_G ratio and mixed acid treatment temperature

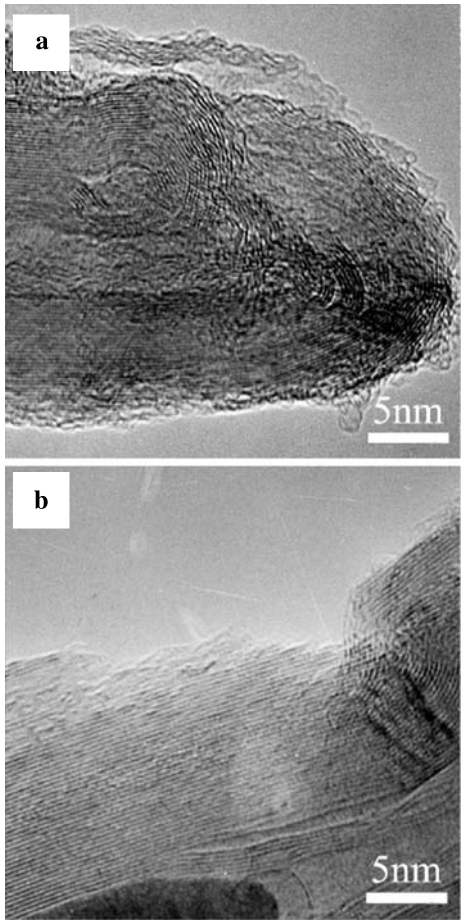

Fig. 5 The HRTEM images of CNTs-120 obtained by mixed acid treatment at 120°C for 0.5 hour. The CNT structure, including the end (**a**) and surface (**b**), was obviously etched by the acid

fection defects, the electrical conductivity also decreased as reported by Zhang et al. [17].

The CNT paper was obtained mostly by simple filtration of CNT pulp. However, the tensile strength of the CNT paper was about 4.3–7.5 MPa, which was much lower than that of SWCNT or double-walled CNT (DWCNT) paper reported by other groups (Table 2). This is far from the good mechanical property of CNT itself as a result of the weak connection among CNTs. Compared with SWCNTs, the MWCNTs obtained by floating catalysis process were of a larger diameter of 40–60 nm, and the distance between MWCNTs was large. Therefore, the van der Waals force between CNTS was not strong. For the potential applications, however, a strong paper is needed. In order to improve the mechanical properties of the produced paper, CNT/polymer composite films were made by various methods, including soaking the CNT paper in a polymer solution and filtering the polymer solution through the CNT paper.

3.2 Enhancing the CNT paper by soaking

A simple way for a polymer to penetrate into paper is soaking the paper into the solution of polymer. In his study, Coleman et al. [46] soaked SWCNT film in PVA solution, which enhanced Young's modulus and strength by three and nine times, respectively. For MWCNT paper, the effects of polymer are obvious. For PEO, it is composed of intramolecule ether groups; PVA has a number of hydroxyl groups, while

Table 3 The mechanical and electrical properties of CNT film obtained by the soaking method

Sample name	Thickness (μm)	Tensile strength (MPa)	Young's modulus (MPa)	Electrical conductivity (S/m)
CNT	96	7.5	785	1.0×10^4
CNT/PEO	143	3.5	323	2.63×10^3
CNT/PVP	125	8.1	787	2.13×10^3
CNT/PVA	132	18.9	1369	1.75×10^3

Table 4 The mechanical and electrical properties of CNT film obtained by vacuum filtration

Sample name	Thickness (μm)	Tensile strength (MPa)	Young's modulus (GPa)	Electrical conductivity (S/m)
CNT	96	7.5	0.785	1×10^4
PVA	100	62.0	4.05	$<10^{-2}$
CNTPVA30min	81	22.8	1.94	0.21×10^4
CNTPVA10h	92	96.1	6.23	0.16×10^4
CNTPVA24h	118	56.9	2.94	8.26×10^2

PVP is full of the carbonyl groups. These polymers were used to enhance the MWCNT paper. The mechanical and electrical properties of CNT composite films obtained by the soaking method are shown in Table 3.

After soaking, the thickness of the CNT paper obviously increased. Among all results, only the mechanical properties of CNT/PVA films were obviously enhanced (Table 3). In fact, the tensile strength and Young's modulus increased from 7.5 and 785 MPa to 18.9 and 1369 MPa, respectively. In contrast, the CNT/PVP films showed little change in properties, while the properties of the CNT/PEO films even decreased. During the soaking process, the polymers diffused into the film and interacted with CNTs to bind them together. PVA easily interacted with functionalized CNTs. Consequently, PVA warped around the CNTs and bound them together. The mechanical properties increased a little for PVP, which had little interaction with CNTs because of the carbonyl groups. As for PEO, the ether groups have little interactions with CNTs. The thickness of CNT films increased as a result of PEO clinging on the CNT paper. The electrical conductivity decreased because these polymers were insulated, and the scattering and block of electrons increased at the interface of the CNT/polymer. However, the tensile strength of the CNT/PVA film increased by 152%, which provided the availability of strong CNT films. It can then be noticed that the polymers, especially PVA, grafted to the surface of CNTs quickly. Then the pores at the surface were blocked up by the polymer, hence the diffusion of polymer into the CNT paper was difficult. This led to the lack of polymer in the inner core of the CNT paper and to the limited improvement in mechanical property.

3.3 Strong CNT/PVA film by vacuum filtration

Wang et al. [47, 48] and Gou et al. [49] fabricated SWNT membranes from a multistep dispersion and filtration method. The membranes were impregnated with epoxy resin/polycarbonate solution to make nanocomposites with a high SWNT loading and improved storage modulus. Vacuum filtration was also used to enhance the mechanical properties while maintaining the electrical properties. Various films were obtained by varying the filtration time.

A group of SEM images (Fig. 6) showed the surface and cross-section of CNT/PVA film fabricated by vacuum filtration. When the filtration lasted for five minutes, although most of the CNTs were coated by PVA, there were still some pores (Fig. 6a). Meanwhile, because of the strong PVA/CNT interaction, the CNT paper shrank, and its thickness decreased from 96 to 81 μm after a 30-minute filtration. With further filtration, more and more of the solution passed through the CNT film, and PVA bonded with CNTs. The thickness of the CNT film increased. A homogeneous CNT/PVA film was formed after a ten-hour filtration (Fig. 6b). Neither pores nor macroscopic defects could be found. Meanwhile, strong interactions between PVA and CNTs were formed, which was confirmed by mechanical property enhancement (see Table 4). After a ten-hour filtration, the tensile strength and Young's modulus reached 96.1 MPa and 6.23 GPa, respectively, or they increased by factors of 12 and 7 compared to those of pristine CNT paper, respectively. At the same time, the electrical conductivity decreased to 0.16×10^4 S/m. When the filtration time increased further to 24 hours, there was too much PVA on the surface of the composite film (Fig. 6c). The fringes of CNTs were not clear (Fig. 6d) except at the end of the cross-section, where short single CNTs were stretched. The thickness increased further; however, the tensile strength and electrical conductivity decreased. The CNT/PVA films obtained by vacuum filtration had a much higher tensile strength and Young's modulus than those obtained by the soaking method. This indicates that vacuum filtration provided an impetus on the diffusion of PVA, then a homogeneous strong film was obtained.

The strongest CNT/PVA film has a tensile strength of 96.1 MPa and Young's modulus of 6.23 GPa. Compared with SWCNT paper/film listed in Table 2, it has good mechanical performance. For a strong CNT film, the stress can be transferred to a single CNT. However, because the mechanism of stress transfer between PVA and CNT was not clear, and the interface was not good, a super strong CNT film was unavailable. Meanwhile, there were still some defects, such as the layered structure as shown in Fig. 2c.

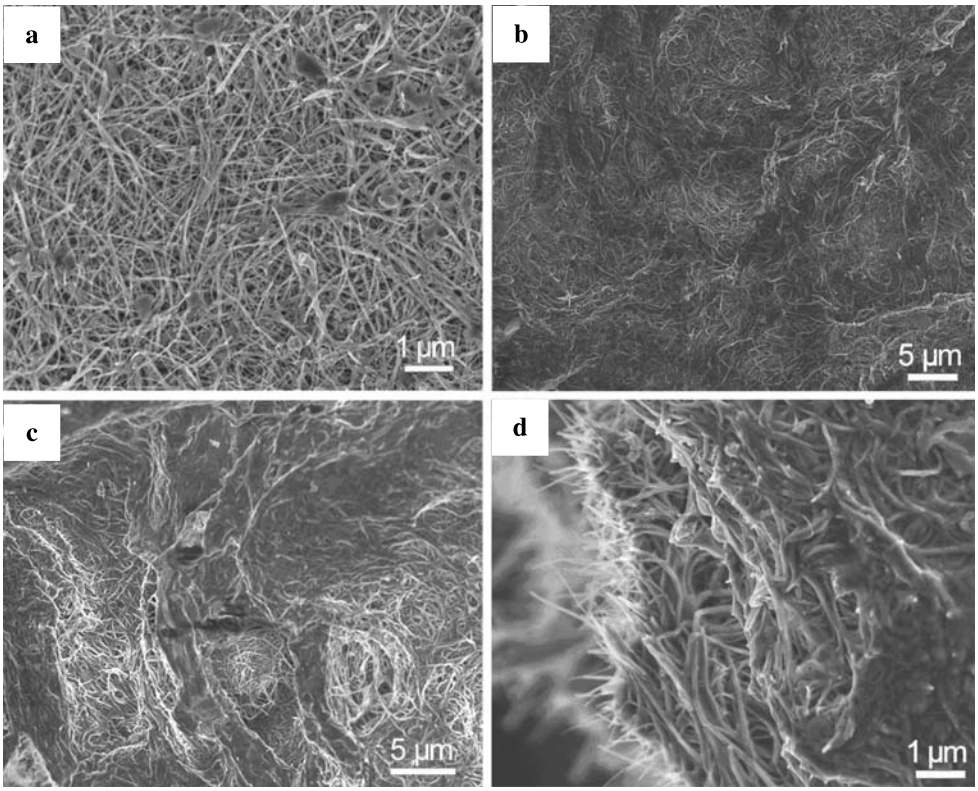

Fig. 6 SEM images of the MWCNT/PVA films. Surface morphologies of MWCNT/PVA films after (**a**) 30-minute, (**b**) 10-hour, and (**c**) 24-hour filtration. (**d**) is the morphology of the cross-section of the film after 24-hour filtration

Therefore, there was still a gap between the theoretical predication and experimental results yielded by this study, thereby encouraging further research on forming a good interface between polymers and CNTs as well as decreasing the defects of CNT composite film. This could open new opportunities in the development of stronger paper/films to meet potential applications.

4 Conclusions

Long VACNT arrays were obtained by synchronous growth in the floating catalysis process. After high-speed shearing, nitric acid and sulfuric acid treatment at various temperatures, and pulping, CNT pulp was obtained which was the solution of long and well-dispersed CNTs. The CNT pulp was filtered to obtain CNT paper. When the treatment temperature was 110°C, due to proper organic group grafting on the surface of CNTs, the tensile strength, Young's modulus, and electrical conductivity were 7.5 MPa, 785 MPa, and 1.0×10^4 S/m, respectively. The CNT paper was further strengthened by making a CNT/polymer composite film.

The CNT paper was soaked in PEO, PVP, and PVA solutions. PVA/CNT film showed the best mechanical properties as shown by the strong interaction between PVA and functionalized CNTs. The tensile strength and Young's modulus increased to 18.9 and 1369 MPa. However, its electrical conductivity decreased. Because polymers could hardly diffuse into CNT paper, vacuum filtration was used to fabricate CNT/PVA film. As a result, PVA penetrated into the CNT paper more, producing a homogeneous CNT/PVA film. After a ten-hour filtration, the tensile strength and Young's modulus of CNT/PVA film were 96.1 MPa and 6.23 GPa, respectively, an obvious increase by factors of 12 and 7 compared to those of pristine CNT paper. However, these properties are not significant compared to those of the individual CNT, making good interactions between polymer and CNTs and low defect density necessary to improve the CNT film further. If this end is materialized, there will be a strong CNT paper/film that could meet the potential applications of CNTs in the future.

Acknowledgements This study was supported by the Foundation for the Author of National Excellent Doctoral Dissertation of P.R. China (No. 200548), the Natural Scientific Foundation of China (No. 20606020), the China National Program (No. 2006CB932702), and the Key Project of the Chinese Ministry of Education (No. 106011).

References

1. W.Z. Li, S.S. Xie, L.X. Qian, B.H. Chang, B.S. Zou, W.Y. Zhou, R.A. Zhao, G. Wang, Science **274**, 1701 (1996)
2. S.S. Fan, M.G. Chapline, N.R. Franklin, T.W. Tombler, A.M. Cassell, H.J. Dai, Science **283**, 512 (1999)
3. F. Wei, Q. Zhang, W.Z. Qian, G.H. Xu, R. Xiang, Q. Wen, Y. Wang, G.H. Luo, New Carbon Mater. **22**, 271 (2007)

4. K.L. Jiang, Q.Q. Li, S.S. Fan, Nature **419**, 801 (2002)
5. R.H. Baughman, C.X. Cui, A.A. Zakhidov, Z. Iqbal, J.N. Barisci, G.M. Spinks, G.G. Wallace, A. Mazzoldi, D. De Rossi, A.G. Rinzler, O. Jaschinski, S. Roth, M. Kertesz, Science **284**, 1340 (1999)
6. M. Endo, H. Muramatsu, T. Hayashi, Y.A. Kim, M. Terrones, N.S. Dresselhaus, Nature **433**, 476 (2005)
7. P.G. Whitten, G.M. Spinks, G.G. Wallace, Carbon **43**, 1891 (2005)
8. M.A. Poggi, P.T. Lillehei, L.A. Bottomley, Chem. Mater. **17**, 4289 (2005)
9. Y.A. Kim, H. Muramatsu, T. Hayashi, M. Endo, M. Terrones, M.S. Dresselhaus, Chem. Vapor Depos. **12**, 327 (2006)
10. A. Kukovecz, R. Smajda, Z. Konya, I. Kiricsi, Carbon **45**, 1696 (2007)
11. F. Zheng, D.L. Baldwin, L.S. Fifield, N.C. Anheier, C.L. Aardahl, J.W. Grate, Anal. Chem. **78**, 2442 (2006)
12. I.P. Kang, M.J. Schulz, J.H. Kim, V. Shanov, D.L. Shi, Smart Mater. Struct. **15**, 737 (2006)
13. Y.A. Kim, H. Muramatsu, M. Kojima, T. Hayashi, Y. Kaburagi, M. Endo, J. Nanosci. Nanotechnol. **6**, 3321 (2006)
14. R. Smajda, A. Kukovecz, Z. Konya, I. Kiricsi, Carbon **45**, 1176 (2007)
15. K.T. Jeng, C.C. Chien, N.Y. Hsu, W.M. Huang, S.D. Chiou, S.H. Lin, J. Power Sources **164**, 33 (2007)
16. J.L. Bahr, J. Yang, D.V. Kosynkin, M.J. Bronikowski, R.E. Smalley, J.M. Tour, J. Am. Chem. Soc. **123**, 6536 (2001)
17. X.F. Zhang, T.V. Sreekumar, T. Liu, S. Kumar, J. Phys. Chem. B **108**, 16435 (2004)
18. J.Q. Wei, H.W. Zhu, Y.H. Li, B. Chen, Y. Jia, K.L. Wang, Z.C. Wang, W.J. Liu, J.B. Luo, M.X. Zheng, D.H. Wu, Y.Q. Zhu, B.Q. Wei, Adv. Mater. **18**, 1695 (2006)
19. T. Gong, Y. Zhang, W.J. Liu, J.Q. Wei, C.G. Li, K.L. Wang, D.H. Wu, M.L. Zhong, Carbon **45**, 2235 (2007)
20. Y. Jia, J.Q. Wei, Q.K. Shu, J.G. Chang, K.L. Wang, Z.C. Wang, J.B. Luo, W.J. Liu, M.X. Zheng, D.H. Wu, Chin. Sci. Bull. **52**, 997 (2007)
21. U. Vohrer, I. Kolaric, M.H. Haque, S. Roth, U. Detlaff-Weglikowska, Carbon **42**, 1159 (2004)
22. S.M. Cooper, H.F. Chuang, M. Cinke, B.A. Cruden, M. Meyyappan, Nano Lett. **3**, 189 (2003)
23. Z.F. Li, G.H. Luo, F. Wei, Y. Huang, Compos. Sci. Technol. **66**, 1022 (2006)
24. V.L. Pushparaj, M.M. Shaijumon, A. Kumar, S. Murugesan, L. Ci, R. Vajtai, R.J. Linhardt, O. Nalamasu, P.M. Ajayan, Proc. Natl. Acad. Sci **104**, 13574 (2007)
25. Y. Wang, F. Wei, G.H. Luo, H. Yu, G.S. Gu, Chem. Phys. Lett. **364**, 568 (2002)
26. Y. Wang, J. Wu, F. Wei, Carbon **41**, 2939 (2003)
27. Q. Zhang, W.P. Zhou, W.Z. Qian, R. Xiang, J.Q. Huang, D.Z. Wang, F. Wei, J. Phys. Chem. C **111**, 14638 (2007)
28. R. Xiang, G. Luo, W. Qian, Y. Wang, F. Wei, Q. Li, Chem. Vapor Depos. **13**, 533 (2007)
29. Q. Zhang, J.Q. Huang, F. Wei, G.H. Xu, Y. Wang, W.Z. Qian, D.Z. Wang, Chin. Sci. Bull. **52**, 2896 (2007)
30. D. Wang, P. Song, C. Liu, W. Wu, S.S. Fan, Nanotechnology **19**, 075609 (2008)
31. W.P. Zhou, Y.L. Wu, F. Wei, G.H. Luo, W.Z. Qian, Polymer **46**, 12689 (2005)
32. W.Z. Qian, T. Liu, F. Wei, H.Y. Yuan, Carbon **41**, 1851 (2003)
33. H. Ago, T. Kugler, F. Cacialli, W.R. Salaneck, M.S.P. Shaffer, A.H. Windle, R.H. Friend, J. Phys. Chem. B **103**, 8116 (1999)
34. P.X. Hou, S. Bai, Q.H. Yang, C. Liu, H.M. Cheng, Carbon **40**, 81 (2002)
35. S. Picozzi, S. Santucci, L. Lozzi, C. Cantalini, C. Baratto, G. Sberveglieri, I. Armentano, J.M. Kenny, L. Valentini, B. Delley, J. Vac. Sci. Technol. A **22**, 1466 (2004)
36. C. Lau, R. Cervini, S. Clarke, M. Markovic, J. Matisons, S. Hawkins, C. Huynh, G. Simon, J. Nanopart. Res. (2008). DOI:10.1007/s11051-008-9376-1
37. J.E. Fischer, H. Dai, A. Thess, R. Lee, N.M. Hanjani, D.L. Dehaas, R.E. Smalley, Phys. Rev. B **55**, R4921 (1997)
38. G.T. Kim, E.S. Choi, D.C. Kim, D.S. Suh, Y.W. Park, K. Liu, G. Duesberg, S. Roth, Phys. Rev. B **58**, 16064 (1998)
39. A.D. Bozhko, D.E. Sklovsky, V.A. Nalimova, A.G. Rinzler, R.E. Smalley, J.E. Fischer, Appl. Phys. A **67**, 75 (1998)
40. T.V. Sreekumar, T. Liu, S. Kumar, L.M. Ericson, R.H. Hauge, R.E. Smalley, Chem. Mater. **15**, 175 (2003)
41. L. Berhan, Y.B. Yi, A.M. Sastry, E. Munoz, M. Selvidge, R. Baughman, J. Appl. Phys. **95**, 4335 (2004)
42. V. Skakalova, A.B. Kaiser, U. Dettlaff-Weglikowska, K. Hrncarikova, S. Roth, J. Phys. Chem. B **109**, 7174 (2005)
43. U. Dettlaff-Weglikowska, V. Skakalova, R. Graupner, S.H. Jhang, B.H. Kim, H.J. Lee, L. Ley, Y.W. Park, S. Berber, D. Tomanek, S. Roth, J. Am. Chem. Soc. **127**, 5125 (2005)
44. P.G. Whitten, A.A. Gestos, G.M. Spinks, K.J. Gilmore, G.G. Wallace, J. Biomed. Mater. Res. B Appl. Biomater. **82**, 37 (2007)
45. L.C. Teague, S. Banerjee, S.S. Wong, C.A. Richter, B. Varughese, J.D. Batteas, Chem. Phys. Lett. **442**, 354 (2007)
46. J.N. Coleman, W.J. Blau, A.B. Dalton, E. Munoz, S. Collins, B.G. Kim, J. Razal, M. Selvidge, G. Vieiro, R.H. Baughman, Appl. Phys. Lett. **82**, 1682 (2003)
47. Z. Wang, Z.Y. Liang, B. Wang, C. Zhang, L. Kramer, Compos. Part A **35**, 1225 (2004)
48. S.R. Wang, Z.Y. Liang, G. Pham, Y.B. Park, B. Wang, C. Zhang, L. Kramer, P. Funchess, Nanotechnology **18**, 095708 (2007)
49. J.H. Gou, Polym. Int. **55**, 1283 (2006)